Detergent-Resistant, Ceramide-Enriched Domains in Sphingomyelin/Ceramide Bilayers

Jesús Sot,* Luis A. Bagatolli,† Félix M. Goñi,* and Alicia Alonso*
*Unidad de Biofísica (CSIC-UPV/EHU) and Departamento de Bioquímica, Universidad del País Vasco, 48080 Bilbao, Spain; and †MEMPHYS-Center for Biomembrane Physics, Department of Biochemistry and Molecular Biology, University of Southern Denmark, Odense, Denmark

ABSTRACT When cell membranes are treated with Triton X-100 or other detergents at 4°C, a nonsolubilized fraction can often be recovered, the ''detergent-resistant membranes'', that is not found when detergent treatment takes place at 37°C. Detergent-resistant membranes may be related in some cases to membrane ''rafts''. However, several basic aspects of the formation of detergent-resistant membranes are poorly understood. To answer some of the relevant questions, a simple bilayer composition that would mimic detergent-resistant membranes was required. The screening of multiple lipid compositions has shown that the binary mixture egg sphingomyelin/egg ceramide (SM/Cer) exhibits the required detergent resistance. In detergent-free membranes composed of different mixtures of SM and Cer (5–30 mol % of Cer) differential scanning calorimetry, fluorescence spectroscopy, and fluorescence microscopy experiments reveal the presence of discrete, Cer-enriched gel domains in a broad temperature range. In particular, at temperatures below SM phase transition ($\approx$ 40°C) two gel (respectively Cer-rich and SM-rich) phases are directly observed using fluorescence microscopy. Although pure SM membranes are fully solubilized by Triton X-100 at room temperature, 5 mol % Cer is also enough to induce detergent resistance, even with a large detergent excess and lengthy equilibration times. Short-chain Cers do not give rise to detergent resistance. SM/Cer mixtures containing up to 30 mol % Cer become fully soluble at ~50°C, i.e., well above the gel-fluid transition temperature of SM. The combined results of temperature-dependent solubilization and differential scanning calorimetry reveal that SM-rich domains are preferentially solubilized over the Cer-rich ones as soon as the former melt (i.e., at ~40°C). As a consequence, at temperatures allowing only partial solubilization, the nonsolubilized residue is enriched in Cer with respect to the original bilayer composition. Fluorescence microscopy of giant unilamellar vesicles at room temperature clearly shows that SM-rich domains are preferentially solubilized over the Cer-rich ones and that the latter become more rigid and extensive as a consequence of the detergent effects. These observations may be relevant to the phenomena of sphingomyelinase-dependent signaling, generation of ''raft platforms'', and detergent-resistant cell membranes.

INTRODUCTION

Membrane rafts were originally proposed as transient microdomains, enriched in sphingolipids and cholesterol (Ch), that would be involved in a variety of processes, including intracellular membrane traffic, cell signaling, and apoptosis (1). In recent years, the term ''raft'' has found widespread use, and sometimes misuse, so that its present definition is rather vague and some further precisions have been required (2,3). The presence of typical ''raft'' lipids in membrane fractions that resist solubilization by Triton X-100 at 4°C (4) led to the operational identification of rafts with these ''detergent-resistant membranes'' (DRMs). At present, the biochemical literature offers hundreds of examples of presumed raft-associated proteins that have been found in detergent-resistant fractions.

However the physicochemical foundations of the detergent-resistance phenomenon are not clear. Studies of model membranes with defined lipid compositions have shown that neither the presence of lipids with a high T_m gel-to-fluid transition temperature (5–7) nor the presence of sphingolipids (8,6) can by themselves explain the resistance. Membrane rafts are considered to exist in the liquid-ordered phase (9,10), and Sáez-Cirión et al. (11) demonstrated that bilayers in the liquid-ordered phase are indeed less prone to solubilization than those in the fluid, or liquid-disordered, phase. An important observation is that the simultaneous presence of sphingomyelin (SM) and Ch, two typical ''raft lipids'', in the bilayers confers on them a high degree of resistance toward detergent solubilization (10,12). Nevertheless, even if the presence of SM and Ch in cell membrane rafts would account for their detergent resistance, a raft property that remains unexplained is that, according to many examples in the literature, these rafts are detergent resistant at 4°C but become solubilized at 37°C. Although it may seem counter-intuitive, fluid lipid bilayers in general, and in particular those containing SM and Ch, are solubilized more easily at lower temperatures (12,6) because at these temperatures the bilayers can accommodate less detergent monomers before breaking down in the form of lipid-detergent mixed micelles (7).

In the search for a simple (if possible binary) mixture of raft-related lipids that would be resistant toward Triton X-100 solubilization at low, but not at high, temperatures we

Submitted June 3, 2005, and accepted for publication October 11, 2005.

Dedicated to the memory of Professor Emilio A. Rivas, a sadly missed colleague and friend.

Address reprint requests to Alicia Alonso, Tel.: 34-94-601 2625; Fax: 34-94-601 3360; E-mail: gbpaliza@lg.ehu.es.

0006-3495/06/02/903/12 $2.00

doi: 10.1529/biophysj.105.067710

have found the SM/ceramide (Cer) system. This work describes the properties of SM/Cer bilayers in the presence of Triton X-100. This simple system may be biologically relevant, because Cer is the end product of SM hydrolysis by sphingomyelinases, and sphingomyelinase activation appears to be at the origin of many cell signaling events (see for reviews Kolesnick et al. (13), Cremesti et al. (14), Goñi and Alonso (15), and Futerman and Hannun (16). Different kinds of vesicles have been used in this study as models for the cell membrane bilayers, namely multilamellar vesicles (MLV), large unilamellar vesicles (LUV), and giant unilamellar vesicles (GUV). Although all of them constitute generally accepted models of biologically meaningful lipid bilayers, each model has its particular advantages, i.e., MLV are convenient to prepare and are not surpassed by any other preparations for calorimetric phase transition studies, LUV are quickly equilibrated with detergents, thus very apt for solubilization studies, and GUV also equilibrate rapidly but have the additional advantage of their large size for microscopy observations. From the point of view of results analysis, all three systems are similar enough to allow generalization of conclusions based on one of them to the other two and, with the usual reservations, to the biological membranes. Our data reveal that Cer-enriched domains that existed in the native bilayer may be considerably modified, in composition and extent, by the detergent during the solubilization process, an observation that casts doubts on the identification of DRMs with physiologically meaningful raft domains.

MATERIALS AND METHODS

Materials

Triton X-100 (regular, batch 48H0208) was purchased from Sigma (St. Louis, MO). Egg-yolk SM (85% C 16:0), egg-yolk Cer (85% C 16:0), *N*-hexanoyl-D-erythro-sphingosine (Cer6), *N*-acetyl-D-erythro-sphingosine (Cer2), and 1,2-dipalmitoyl-*sn*-phosphocholine (DPPC) were supplied by Avanti Polar Lipids (Alabaster, AL) and were used without further purification. Egg-yolk phosphatidylcholine (containing 35% C 16:0, 32% C 18:1, 18% C 18:2, and 16% others) was grade I from Lipid Products (South Nutfield, England). 2,2,6-tetramethyl-1-piperidinyloxy (TEMPO, free radical, sublimed, 99%) was from Sigma-Aldrich (St. Louis, MO). 1,1′-Dioctadecyl-3,3,3′3′-tetramethylindocarbocyanine perchlorate (DiI), 1,6-diphenyl-1,3,5-hexatriene (DPH), and 2-dimethylamino-6-lauroylnaphthalene (Laurdan) were from Molecular Probes (Eugene, OR). All other reagents were of analytical grade.

MLV preparation

For MLV liposome preparation SM or occasionally other phospholipids and Cer were dissolved in chloroform/methanol (2:1, v/v), and the mixture was evaporated to dryness under a stream of nitrogen. Traces of solvent were removed by evacuating the samples under high vacuum for at least 2 h. The samples were hydrated at 45°C in 20 mM PIPES, 150 mM NaCl, 1 mM EDTA, pH 7.4, helping dispersion by stirring with a glass rod. To ensure homogeneous dispersion the hydrated samples were extruded between two syringes through a narrow tubing (0.5 mm internal diameter, 10 cm long) 100 times at 45°C. In these samples the amount of phospholipid was kept constant, whereas the amount of Cer and, correspondingly, that of total lipid varied. The final phospholipid concentration was measured in terms of lipid phosphorous, as described previously (5,6). Liposome suspensions were mixed with the appropriate detergent solutions to obtain the desired detergent/lipid (D/L) ratio. Final lipid concentration was always 1 mM. The mixtures were left to equilibrate (30 min for the preliminary observations or 24 h for equilibrium conditions), and solubilization was assessed from the changes in turbidity.

Solubilization assays

Solubilization was assayed using either the turbidity or the centrifugation methods. The turbidity method (17) is based on the decrease in suspension turbidity that accompanies the lamellar-to-micellar transition. Turbidity was measured as absorbance at 500 nm in a Uvikon 922 spectrophotometer (Kontron, Regensdorf, Switzerland) equipped with thermoregulated cell holders. The turbidity values were normalized by setting 100% as the turbidity of the vesicle suspension without detergent, whereas 0% turbidity corresponded to pure buffer.

In the centrifugation assay of liposome solubilization, the nonsolubilized fraction after detergent treatment was separated from the micelles by centrifugation (14,500 $\times$ g, 20 min) in a standard Eppendorf centrifuge at room temperature. For quantitative analysis of the lipid compositions in the nonsolubilized membranes, the pellets were extracted with chloroform/methanol (2:1). The organic phase was concentrated and separated on thin-layer chromatography Silica Gel 60 plates, with chloroform/methanol/water (50:42:1, by volume). After charring the organic phase with a sulfuric acid reagent, the spot intensities of both SM and Cer were quantified using a Bio-Rad (Hercules, CA) GS-800 Calibrate Densitometer with the Quantity One software from Bio Rad.

Fluorescence quenching experiments

Quenching of the DPH fluorescence by TEMPO was measured as follows. Lipids, DPH, and (when required) TEMPO were mixed at a 300:1:1 ratio in organic solvent, then the solvent was evaporated, and the mixture was vacuum dried for at least 2 h in the dark. The vesicles were prepared in 20 mM PIPES, 150 mM NaCl, 1 mM EDTA, pH 7.4 as described above. Vesicles with and without TEMPO were prepared for all SM/Cer ratios. Fluorescence quenching was recorded in a SLM-AMINCO 8100 spectrofluorometer (Jobin Yvon, Longjumeau, France) equipped with thermoregulated cell holders. DPH fluorescence was excited at 360 nm; emission was recorded at 428 nm.

Differential scanning calorimetry experiments

For the differential scanning calorimetry (DSC) measurements both lipid suspensions and buffer were degassed before being loaded into the sample or reference cell of an MC-2 high-sensitivity scanning calorimeter (MicroCal, Northampton, MA). The final phospholipid (usually SM) concentration in the samples was 1 mM. Three heating scans, at 45°C/h, were recorded for each sample. Lipid phosphorous assays were carried out on all SM-containing samples after the DSC scans to obtain accurate ΔH values (in kcal/mole of phospholipid). Thermogram transition temperatures, enthalpies, and widths at half-height were determined using the software ORIGIN (Microcal) provided with the calorimeter. Complex thermograms suggesting more than one underlying transition were resolved mathematically into the number of necessary peaks, usually three, assuming independent transitions, so that the sum of these constituents gave the best fit to the original data. For curve fitting, the software GRAMS_32 Spectra Notebase (Galactic Industries, Salem, NH) was used (www.thermo.com/eThermo/CMA/PDFs/Product/productPDF_24179.pdf).

Giant vesicle preparation

GUV composed of egg SM/egg Cer mixtures were prepared as described previously, using the electroformation method originally developed by

Angelova and Dimitrov (18). A previously described special temperature controlled chamber (19,20) was used for this purpose. Briefly, the process can be described in three steps: 1), ≈3 μl of the stock solution of lipid organic solution (0.2 mg/ml premixed with the fluorescent probe at 0.5 mol %) were spread on the surface of each Pt wire. The chamber was located under a stream of N_2 during this procedure and then placed under vacuum overnight to remove the organic solvent; 2), aqueous solution was added to the chamber (a 200 mOsm sucrose solution prepared with Millipore-filtered water 17.5 MΩ/cm). The sucrose solution was previously heated to the desired temperature (above the lipid mixture phase transition, ~68°C) and then sufficient volume was added to cover the Pt wires (≈300 μl); and 3), the Pt wires were connected immediately to a function generator (Digimess Fg 100 plug-In, Eichenau, Germany), and a low frequency alternating current (AC) field (sinusoidal wave function with a frequency of 10 Hz and an amplitude of 3 V) was applied for 120 min. After vesicle formation, the AC field was turned off and the vesicles were collected with a pipette and transferred to a plastic tube.

Observation of giant vesicles

Aliquots of giant vesicles suspended in sucrose were added to an equiosmolar concentration of glucose solution. Due to the density difference between the two solutions, the vesicles precipitate at the bottom of the chamber, which facilitates observation of the GUV in the inverted fluorescence microscope. GUV preparations were observed in 8-well plastic chambers (Lab-tek Brand Products, Naperville IL). The chamber was located in an inverted confocal/two photon excitation fluorescence microscope (Zeiss, Karlsruhe, Germany) LSM 510 META NLO) for observation. The Ti:Sa laser used for two photon excitation mode was a MaiTai XF-W2S (Broadband Mai Tai with 10 W Millennia pump laser, tunable excitation range 710–980 nm, Spectra Physics, Mountain View, CA). The excitation wavelengths were 543 nm (for DiI_{C18} in one photon excitation mode) and 780 nm (for Laurdan in two photon excitation mode). The images were simultaneously collected in two different channels using band-pass filters of 590 ± 25 nm and 424 ± 37 nm for DiI_{C18} and Laurdan, respectively. All these experiments were performed at room temperature (25°C).

RESULTS

Preliminary observations

For a preliminary screening of detergent-resistant lipid membranes, a series of experiments was performed in which suspensions of phospholipid vesicles (MLV) are treated with aliquots of a concentrated solution of Triton X-100 at room temperature with constant stirring. Suspension turbidity was recorded 30 min after detergent addition. Although these conditions do not guarantee the complete equilibration of the systems under study, the procedure is useful for the fast screening of the solubilization properties of different lipid membranes. MLV containing pure phospholipids are fully solubilized (i.e., turbidity or A_{500} became <5% of the original) in all cases at total D/L mole ratios ≤3.5 (Fig. 1). Of the various binary lipid compositions tested, those containing SM and Ch at various proportions are markedly resistant toward detergent solubilization, as expected from previous studies (6,12) (data not shown). More interesting is the observation that egg Cer, in mixtures with SM or with DPPC but not with egg PC, also gives rise to detergent-resistant lipid membranes (Fig. 1). Note that in these experiments, both pure egg SM and pure DPPC require for their full

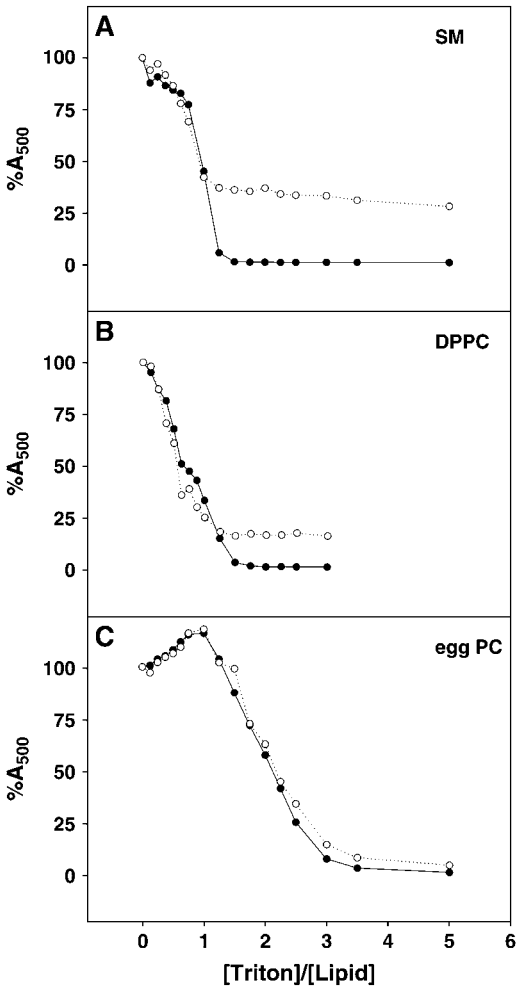

FIGURE 1 Vesicle solubilization by Triton X-100 under near-equilibrium conditions: effect of Cer. Solubilization was measured as a decrease in vesicle suspension turbidity (A_{500}). Detergent was added to the vesicle suspension, with constant stirring, and left to equilibrate for 30 min at room temperature. Lipid concentration was 1 mM. MLV composition: egg SM (*A*), DPPC (*B*), and egg phosphatidylcholine (*C*), with (○) or without (●) 10 mol % egg Cer.

solubilization less detergent than pure egg PC, also in agreement with our previous observations (6). In view of the results in Fig. 1 and other similar studies, an exhaustive study of the SM/Cer system has been undertaken. This study has been performed because i), SM/Cer mixtures are formed in cell membranes as a result of sphingomyelinase action with important physiological consequences (see reviews by Kolesnick et al. (13), Cremesti et al. (14), and Marchesini and Hannun (21)), and ii), because SM/Cer mixtures are resistant to detergent solubilization at room temperature. Additionally, some DPPC/Cer mixtures have also been studied.

Solubilization studies under equilibrium conditions

Detergent solubilization of lipid membranes may sometimes be a very slow process, with ''kinetic traps'' giving rise to

pseudoequilibrium situations (3,7). For this reason MLV composed of egg SM and various proportions of egg Cer have been incubated with Triton X-100 at a D/L = 20 for 24 or 48 h at room temperature and the suspension turbidity measured afterwards. As seen in Fig. 2, resistance toward solubilization increases with the proportion of egg Cer in the bilayers, thus confirming the preliminary observations in Fig. 1 *A*. Virtually identical results are obtained after 24 or 48 h, suggesting that 24 h allow full equilibration of the system. Consequently, all further measurements have been made after 24 h.

In a previous study we have shown that, under conditions of partial solubilization of heterogeneous lipid membranes, the nonsolubilized fraction appears enriched in certain components (6). To test whether or not this is the case with the SM/Cer system, control and detergent-treated MLV (D/L = 20) containing Cer in various proportions are left to equilibrate for 24 h and then centrifuged in an Eppendorf centrifuge at 14,500 × *g* for 20 min at room temperature. Previous experiments had shown a good correlation between the amount of lipid recovered in the supernatant under these conditions and the decrease in turbidity that is commonly taken as a measure of solubilization. As expected the total amount of lipid recovered in the pellets is larger in the control than in the detergent-treated samples (data not shown). The proportion of Cer in the pellets has been quantitatively analyzed, with the results shown in Fig. 3, namely that the pellets of the detergent-treated samples are enriched in Cer over the control vesicles. Thus the lipid membranes are not homogeneously solubilized under these conditions, Cer being less prone to incorporation into lipid-detergent mixed micelles than SM.

The specificity of the phenomenon of detergent resistance with respect to Cer chain length and phospholipid species has been tested under equilibrium conditions, and the results are summarized in Fig. 4. Synthetic ''short-chain Cers'', i.e., *N*-acetylsphingosine (Cer2) and *N*-hexanoylsphingosine (Cer6) do not give rise to DRM (Fig. 4 *A*). In fact, solubilization is even better in the presence of 30 mol % of these two compounds, whose detergent properties are known (22,23). Note that egg Cer contains mainly palmitic (C16) acid (see Materials and Methods). With respect to phospholipid species and in agreement with the results in Fig. 1, DPPC (but not the unsaturated egg PC) supports detergent resistance. This last phenomenon appears to be strongly associated to the presence of long, saturated fatty acyl chains, both in the phospholipids and the Cer. Note that egg Cer, i.e., the end product of SM degradation by sphingomyelinase, is very effective in the formation of DRM when mixed with its parent phospholipid.

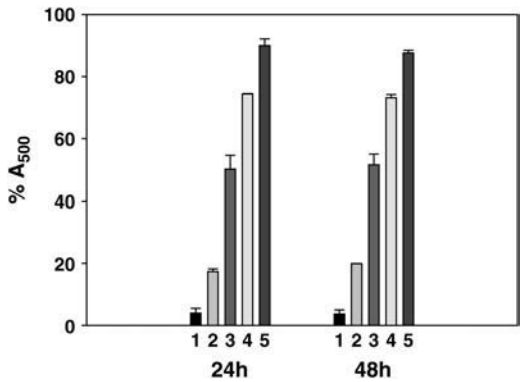

FIGURE 2 Vesicle solubilization by Triton X-100 under equilibrium conditions: effect of Cer. Solubilization was measured as a decrease in vesicle suspension turbidity (A_{500}). Lipid concentration was 1 mM. Detergent: lipid/mole ratio was 20:1. Solubilization was allowed to proceed for either 24 h or 48 h at room temperature. MLV composition: egg SM (*column 1*), + 5 mol % egg Cer (*column 2*), + 10 mol % egg Cer (*column 3*), + 20 mol % egg Cer (*column 4*), + 30 mol % egg Cer (*column 5*). Data are average values ± SD ($n = 3$).

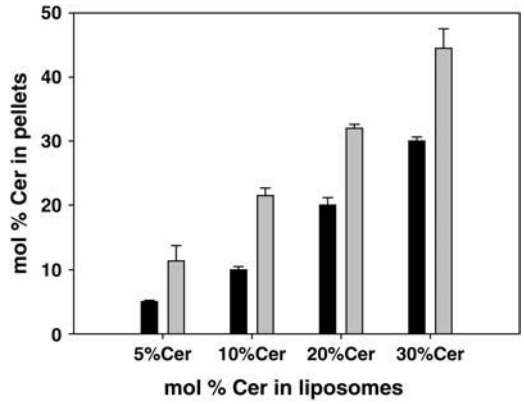

FIGURE 3 Cer proportions in the nonsolubilized fractions. The nonsolubilized fractions after 24 h detergent treatment (D/L ratio 20:1) were collected by centrifugation, and their SM and Cer concentrations quantitated. Cer proportions in the pellets (*shaded*) are shown in the figure as a function of the nominal Cer concentration in the original MLV. The proportions of Cer in the pellets from untreated vesicles (*solid*) are shown for comparison. Data are average values ± SD ($n = 3$).

DRM are often isolated from cells treated with Triton X-100 at 4°C, whereas the same treatments at 37°C produce complete solubilization (4). For this reason the effect of temperature on the solubilization of SM/Cer vesicles has been tested. Both detergent incubation and turbidity measurements are carried out at the temperatures indicated in Fig. 5. The results in panel *A* are obtained by mixing detergent and MLV (D/L = 20) at 27°C. After 20 min, temperature is increased at a rate of ~45°C/h up to 57°C and A_{500} recorded. Solubilization increases markedly above ~40°C, i.e., the gel-fluid transition temperature of egg SM (24,25). Results in Fig. 5 *B*, obtained after 24 h equilibration, indicate that also under these conditions solubilization increases with temperature. Note in particular that at 4°C all samples exhibit very low solubility. Almost identical results are obtained when extrusion LUV (~100 nm in diameter) are used instead of MLV.

The relationship between solubilization and temperature, and the fact that egg Cer tends to give rise to Cer-enriched

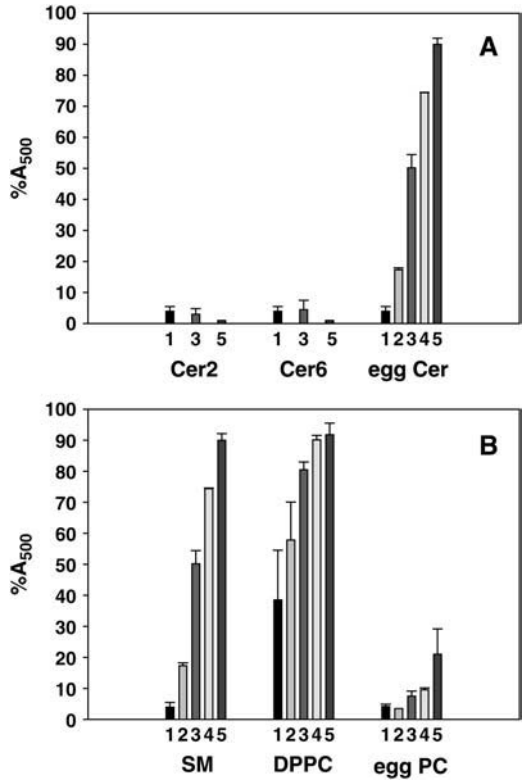

FIGURE 4 Effect of hydrocarbon chains in the phenomenon of detergent resistance. Solubilization and other conditions as in Fig. 2. Solubilization time was 24 h. (*A*) Effect of Cer N-acyl chain length: acetyl (Cer2), hexanoyl (Cer6), or predominantly hexadecanoyl (egg Cer). (*B*) Effect of phospholipid chain unsaturation: egg SM, DPPC, and egg phosphatidylcholine (egg PC). Cer proportions, in mol %: 0 (*column 1*), 5 (*column 2*), 10 (*column 3*), 20 (*column 4*), and 30 (column 5). Data are average values ± SD ($n = 3$).

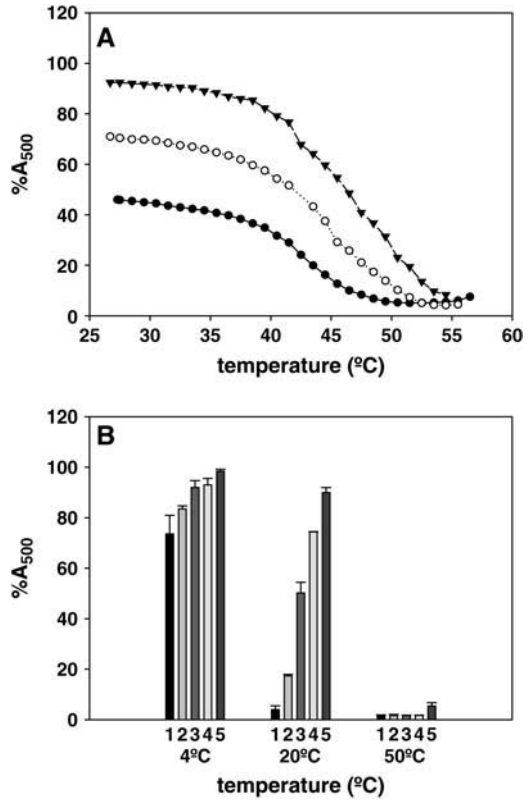

FIGURE 5 Effect of temperature on the solubilization of SM/Cer mixtures by Triton X-100. Solubilization and other conditions as in Fig. 2. (*A*) Solubilization as a function of temperature. MLV composed of egg SM + 10 mol % egg Cer (●), + 20 mol % egg Cer (○), + 30 mol % egg Cer (▼). (*B*) Solubilization at selected temperatures. Cer proportions in mol %: 0 (*column 1*), 5 (*column 2*), 10 (*column 3*), 20 (*column 4*), and 30 (*column 5*). Data are average values ± SD ($n = 3$).

domains in mixtures with phosphatidylcholine or phosphatidylethanolamine (26,27, and references therein), prompted us to explore the effect of Cer on the gel-fluid lamellar phase transition of SM. The results are summarized in Fig. 6. Pure egg SM displays a rather narrow transition centered at 39°C (Fig. 6 *A*). However the presence of egg Cer, even at low proportions, has the effect of widening the phase transition, shifting it to higher temperatures, with little change in the onset temperature. The clearly asymmetric shape of the endotherms suggests the formation of high-*T* melting SM/Cer domains. In fact the observed overall endotherms can be fitted to three component endotherms (*dotted lines* in Fig. 6 *A*) corresponding to as many coexisting domains with different compositions. In principle, the Cer-dependent shift of the thermotropic transition toward higher temperatures is expected because the pure egg Cer contains mainly palmitic acid and palmitoyl-Cer (*N*-palmitoylsphingosine) displays an endothermic phase transition at 93°C (28,29).

From the thermograms in Fig. 6 *A*, a partial phase diagram (or temperature-composition diagram) can be constructed (Fig. 6 *B*). It is rather similar to those published for DPPC/Cer (29) and dielaidoyl(di-*trans*-octadecenoyl)phosphatidylethanolamine/Cer (27) mixtures. The fact that the onset temperature (*filled circles* in Fig. 6 *B*) varies little with Cer concentration indicates low miscibility of Cer with SM in the gel (or L_β) phase. At these low temperatures a Cer-enriched crystalline phase C coexists with an SM-rich gel phase L_β. On the contrary, the progressive increase in completion temperature of the transition in the presence of Cer (*empty circles* in Fig. 6 *B*) suggests that Cer becomes miscible with SM in the fluid (or L_α) phase. In the presence of Cer, in the temperature range between the onset and completion of the phase transition at least three domains coexist, as indicated by the complex, asymmetric thermograms.

The presence of coexisting domains with different degrees of fluidity in SM/Cer bilayers, within a wide range of temperatures, as shown by the calorimetric results in Fig. 6, is further confirmed using a very different technique, namely fluorescence spectroscopy. To this aim the SM/Cer lipid membranes are doped with a small proportion of the fluorescent probe DPH. This probe is known to distribute uniformly over domains either in the gel or in the fluid phase (30). DPH fluorescence is recorded as a function of temperature both in the absence and in the presence of TEMPO, a spin probe that

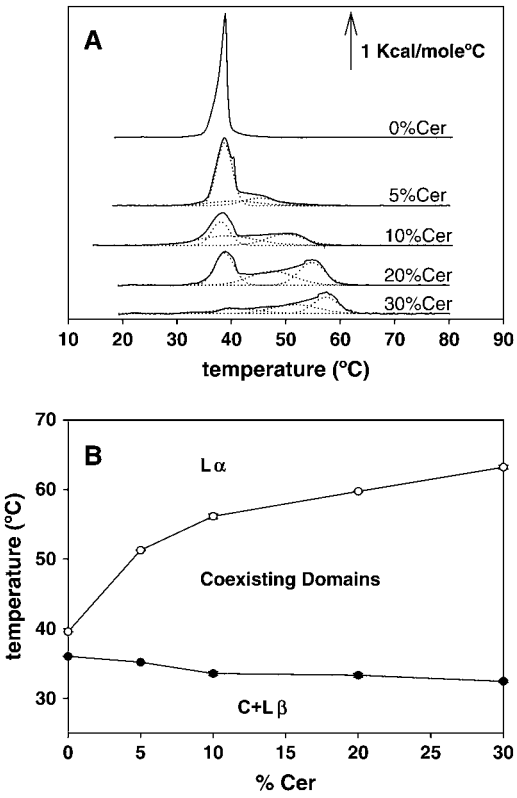

FIGURE 6 DSC of SM/Cer vesicles. (*A*) Representative thermograms. The proportion of Cer, in mol %, is indicated for each thermogram. Dotted lines correspond to the decomposition of the overall endotherm into three symmetrical components. (*B*) Temperature-composition diagram derived from calorimetric measurements as shown in the above panel. C, Cer-rich crystalline phase; L_β, gel phase; L_α, fluid (liquid disordered) phase.

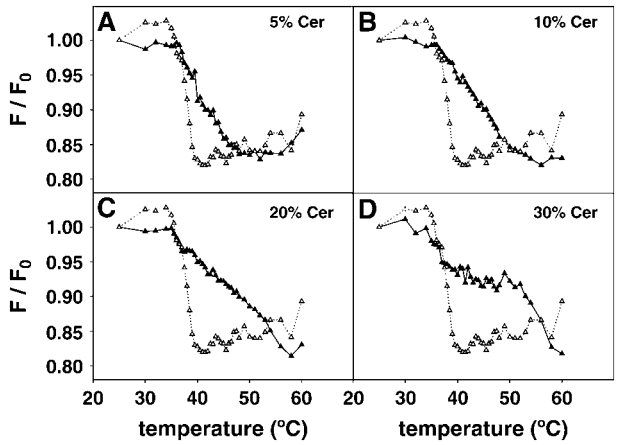

FIGURE 7 Fluorescence quenching demonstration of the presence of ordered domains in SM/Cer mixtures. The fluorescent probe DPH partitions evenly into the different domains, whereas the quencher TEMPO partitions preferentially into the disordered domains. Fluorescence quenching is expressed as a function of temperature as *F*/*F*o (DPH fluorescence intensity in the presence/in the absence of TEMPO). *F*/*F*o at 22°C is normalized to 1.0. A decreased *F*/*F*o indicates the melting of ordered domains. (Δ) Pure SM. (▲) + Cer, as indicated in each panel.

partitions into the disordered, but not into the ordered, domains in lipid membranes. When all membrane components are in the gel phase, TEMPO is largely in the aqueous medium. TEMPO has the effect of quenching DPH fluorescence. As a consequence, in the presence of TEMPO, DPH fluorescence arises mainly from the more ordered domains, and the *F*/*F*o ratio of fluorescence emission ''in the presence/in the absence'' of TEMPO should provide information on the existence of ordered domains in the membranes. The results as a function of temperature are shown in Fig. 7 for pure SM (*empty triangles*) and for various SM/Cer mixtures. For all mixtures at 25°C, quenching by TEMPO is very small because the lipids are in the gel (solid-ordered) phase at that temperature. DPH fluorescence (expressed as the *F*/*F*o ratio) is set at 1.0 under those conditions. For pure SM, increasing *T* up to ~33°C leads to a decrease in quenching (i.e., an increase in *F*/*F*o), presumably due to a thermal increase in internal conversion (31) unrelated to phase effects. Above 33°C, with the onset of the phase transition, TEMPO begins partitioning into the lipid membranes, and consequently quenching rises and *F*/*F*o decreases steeply. A minimum is reached at ~40°C, i.e., when only the fluid-disordered L_α phase exists (Fig. 6). At higher temperatures thermal effects again cause a slight decrease in quenching.

When Cer is present, even at low proportions, a small fraction is incorporated into the gel phase, as shown in the phase diagram (Fig. 6, *solid symbols*) presumably causing some degree of disordering, just as Ch disorders DPPC bilayers in the gel phase (32). The decreased order allows some TEMPO to partition, so that quenching is higher (*F*/*F*o is lower) for all SM/Cer mixtures than for pure SM at $T <$ 35°C. Lipid melting above 35°C is accompanied by an increased quenching in all the SM/Cer mixtures (Fig. 7, *A–D*). Quenching in these mixtures (lowering of *F*/*F*o) extends to temperatures beyond those observed for pure SM, because the transition is widened toward the high-*T* side in the presence of Cer (Fig. 6).

A direct comparison of the solubilization, calorimetric, and fluorescence measurements provides additional insights into the process. An example is shown in Fig. 8, where DSC, fluorescence quenching, and solubilization data for the 10% Cer sample are jointly presented as a function of temperature. Five different temperature regions can be distinguished, the various techniques showing good agreement within ±1–2°C. The high-*T* boundaries of regions 2, 3, and 4 correspond to the thermotropic transition end-points for the three components observed in the DSC endotherm. Note that in DSC and solubilization experiments samples have been heated at the same rate (45°C/h), whereas fluorescence measurements have been performed under equilibrium conditions. This may explain small differences in the boundaries between the various regions, as detected through the different techniques. Region 1 (below 35°C) corresponds mainly to the rather featureless gel phase. Region 2 (35°C–41°C) witnesses

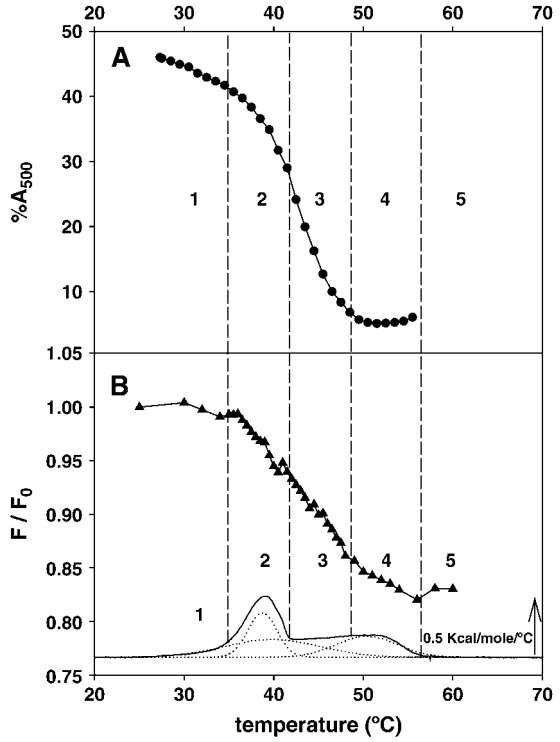

FIGURE 8 Temperature-dependent solubilization and domain melting in SM vesicles containing 10 mol % Cer. (*A*) Triton X-100 solubilization, redrawn from Fig. 5. (*B*) (▲) Melting of domains, redrawn from Fig. 7 *B*. Solid line: thermogram, redrawn from Fig. 6 *A*.

a rather cooperative calorimetric transition, corresponding probably to the melting of SM-rich domains, with the concomitant steep increase in DPH quenching by TEMPO (decrease in *F*/*F*o). Solubilization increases at this stage. Region 3 (41°C–49°C) is characterized by a small change in C_P (DSC signal) and a continued decrease in *F*/*F*o. The simplest interpretation is that, in this temperature range, low-cooperativity melting is taking place, i.e., melting of small domains. Low cooperativity is at the origin of the small change in C_P; however, melting is shown by the decrease in *F*/*F*o. It is interesting that a large increase in solubilization occurs within this temperature range, i.e., as soon as the highly cooperative SM-rich domains are melted (together with some melting of Cer-enriched domains). Region 4 (49°C–57°C) corresponds to the completion of the melting of Cer-enriched domains. Solubilization is also completed at this stage. (Turbidity does not decrease any further, and it may even increase because of the ''cloud point'' of Triton X-100 near 55°C.) *F*/*F*o continues to decrease, albeit less steeply. Finally, in region 5 (above 57°C) when the bilayer is in the pure L_α (fluid) phase, no further effects are detected.

Fluorescence microscopy studies

An additional series of observations has been carried out on GUV at room temperature using fluorescence microscopy. Representative images of DiI_{C18}-labeled GUV of different compositions are shown in Fig. 9. Pure SM vesicles appear uniformly stained, whereas those containing egg Cer display dark areas. Increasing Cer concentration (Fig. 9) leads to a parallel increase in dark areas that change their shape from circular to elongated or worm-like. The increase in dark areas with increasing Cer concentration strongly supports the idea that DiI_{C18} (in this particular mixture) is segregated from Cer-rich areas. For this mixture Cer-enriched domains are detected at low Cer concentration, in agreement with the report by Carrer and Maggio (29). These authors have observed Cer-rich domain formation with as little as 3% Cer in DPPC bilayers, based on DSC experiments. The percolation point for the Cer-rich domains appears to occur between 20% and 30% Cer, at the latter concentration the ''dark'' domain being already continuous. Note that a certain degree of heterogeneity was observed in the pattern of dark and bright domains even for vesicles of the same average composition, but the ones shown in Fig. 9 correspond by far to the most abundant species for a given composition.

Triton X-100 solubilization of GUV can be observed in real time under the fluorescence microscope. Representative examples are presented in Fig. 10. These experiments were performed at room temperature. Note, from the data in Fig. 5, that only partial solubilization is observed under these conditions. In general, solubilization causes fluorescence emission to become weaker, and eventually the vesicle shrinks and, for low Cer concentrations, becomes undetectable. Intensity of the yellow color has been quantified as a function of time, and it is found to decrease gradually, suggesting a concomitant lipid solubilization (data not shown). When looking at vesicle areas where dark and bright

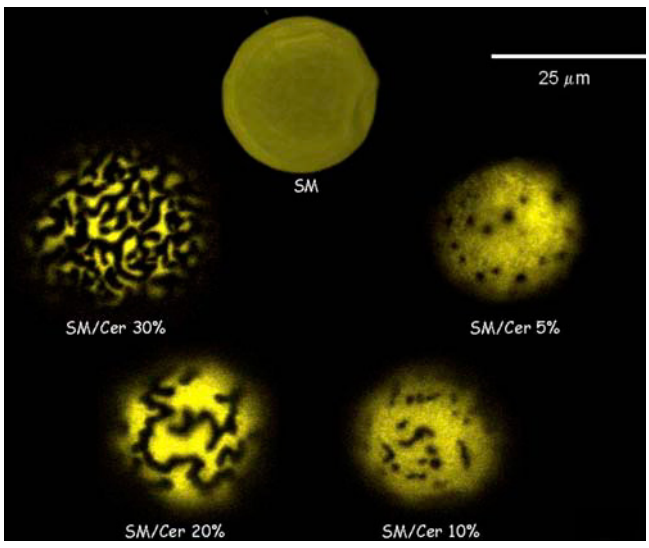

FIGURE 9 Cer-rich domains in GUV composed of SM/Cer. Images obtained by fluorescence microscopy of DiI-stained vesicles. DiI partitions preferentially into the less ordered domains. Room temperature.

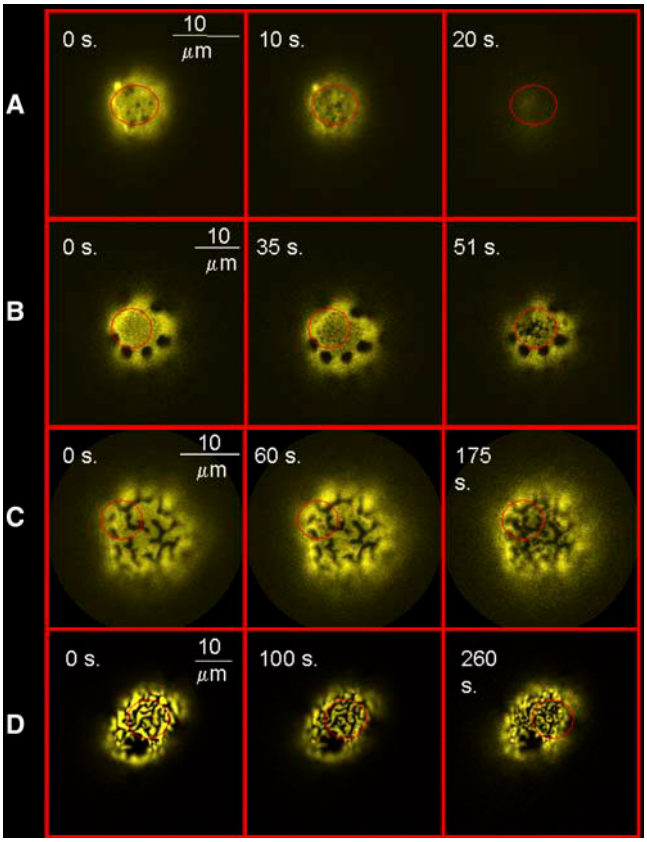

FIGURE 10 Time course of the partial solubilization of sphingomyelin/Cer GUV by Triton X-100 at room temperature. Fluorescence microscopy of DiI-stained vesicles. Times after detergent addition are indicated for each picture. Rows *A–D* correspond to vesicles containing 5, 10, 20, and 30 mol % Cer, respectively.

domains coexist, e.g., those contained within red circles in Fig. 10, the dark areas are seen to remain more or less undisturbed, whereas the bright areas darken in turn. This is interpreted in terms of preferential solubilization of SM-rich domains, whereas a detergent-resistant, Cer-enriched, ''dark'' residue is left behind. Note also that the solubilization process takes considerably longer for the Cer-rich vesicles (i.e., compare the times at the right-hand side stack of images in Fig. 10). The resistance of Cer-rich domains to detergent solubilization is in agreement with the data in Fig. 3.

A more detailed view of single vesicle solubilization and formation of Cer-enriched DRM can be obtained with double-stained vesicles. Fig. 11 depicts a GUV containing 10% Cer labeled with DiI_{C18} (pseudocolor *yellow*) that partitions preferentially into SM-rich domains and Laurdan (pseudocolor *red*) that shows an enhanced fluorescence emission in the Cer-rich domains. Note that the photoselection effect (33) precludes observing Laurdan fluorescence in the GUV polar region. When double-stained vesicles are observed by confocal microscopy, the images reveal significant changes at the equatorial plane of the vesicles. Examples of the solubilization of 10% and 20% Cer-containing GUV are shown respectively in Figs. 12 and 13. In both cases the vesicles are seen to shrink as solubilization proceeds. In addition, the yellow-stained SM-rich domains fade gradually (see pictures marked D), whereas the red, Cer-rich domains (marked L) that were hardly visible at time 0 (particularly for the 10% Cer vesicles, Fig. 12) become more discrete, detectable structures. Cer-rich domains present a flat, rigid appearance, contributing to the characteristic shape of the vesicles at an advanced stage of solubilization, in which the equatorial contour consists of alternating straight and convoluted segments, the latter corresponding to remaining SM-rich domains. The Laurdan-stained Cer-rich domains in Figs. 12 and 13 correspond to the dark, non-DiI_{C18}-labeled domains in Figs. 9 and 10. In summary, the fluorescence micrographs confirm the above conclusions that Triton X-100 at room temperature solubilizes preferentially SM-rich domains and that the DRM are enriched in Cer.

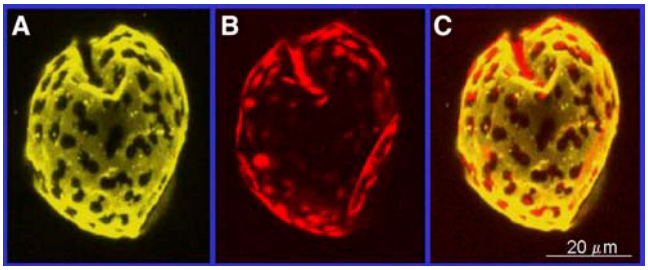

FIGURE 11 Fluorescence microscopy. Double staining of a GUV composed of SM/Cer (80:20 mol ratio). DiI (pseudocolor *yellow*) stains preferentially the less ordered, SM-rich domains. Laurdan (pseudocolor *red*) stains preferentially the more ordered, Cer-rich domains.

DISCUSSION

The above experimental data demonstrate that i), Cer gives rise to Cer-rich domains in binary mixtures with SM, ii), Cer-rich and -poor domains coexist well above the gel-fluid transition temperature of SM (~40°C), iii), the Cer-enriched domains are detergent resistant, and iv), the nonsolubilized residue is enriched in Cer over the original bilayer composition. We shall briefly comment on these results and then examine their possible implications for cell biology studies.

Cer domains

Formation of Cer-rich domains (Figs. 6–9) due to poor mixing of Cer and SM does not come as a surprise, since it has already been demonstrated by Massey (34) using fluorescence probe techniques. Cer-rich domains have also been observed in glycerophospholipid membranes with a variety of techniques (26,29,35–37). Carrer and Maggio (29) have

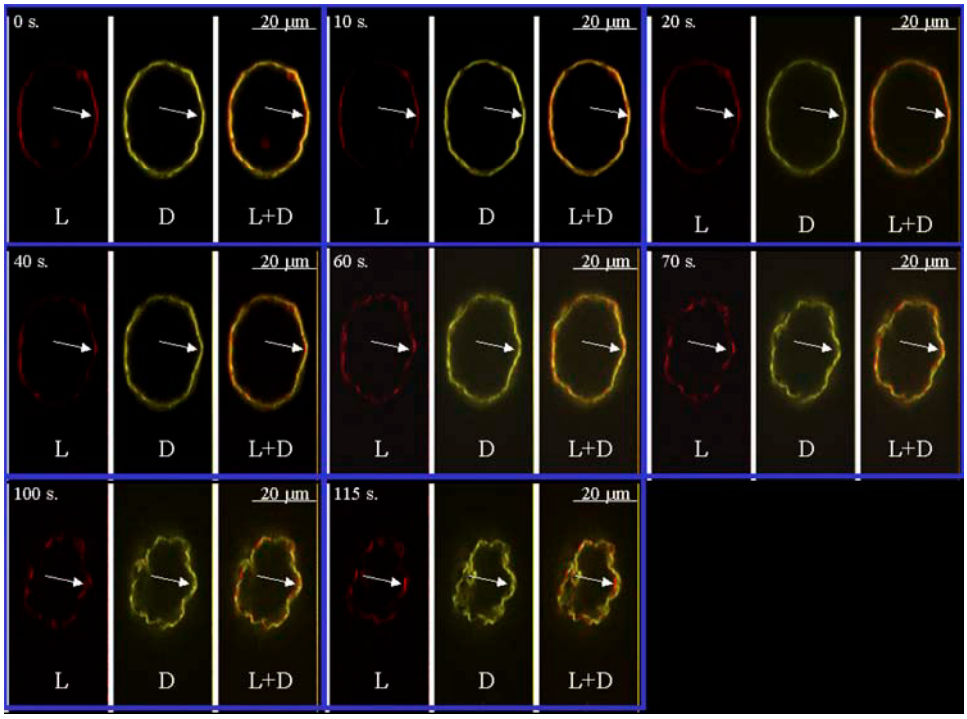

FIGURE 12 Confocal fluorescence microscopy. Time course of the partial solubilization of double-stained vesicles containing 10 mol % Cer. The equatorial planes are shown. Each set of three images contains, respectively, the Laurdan-excited fluorescence (*L*), the DiI fluorescence (*D*), and the corresponding overlap (*L*+*D*). Times after detergent addition are given in seconds. Room temperature. The arrows point to the formation of a large Cer-enriched domain.

noted the coexistence of two gel phases differing in Cer concentration. However the coexistence of domains well above the gel-fluid transition temperature of SM (Figs. 6–8) has not been previously detected in SM/Cer binary mixtures to our knowledge. Domain coexistence in glycerophospholipid-Cer mixtures above the main transition temperature of the glycerophospholipid has been observed by Holopainen et al. (38) and by Hsueh et al. (37), among others.

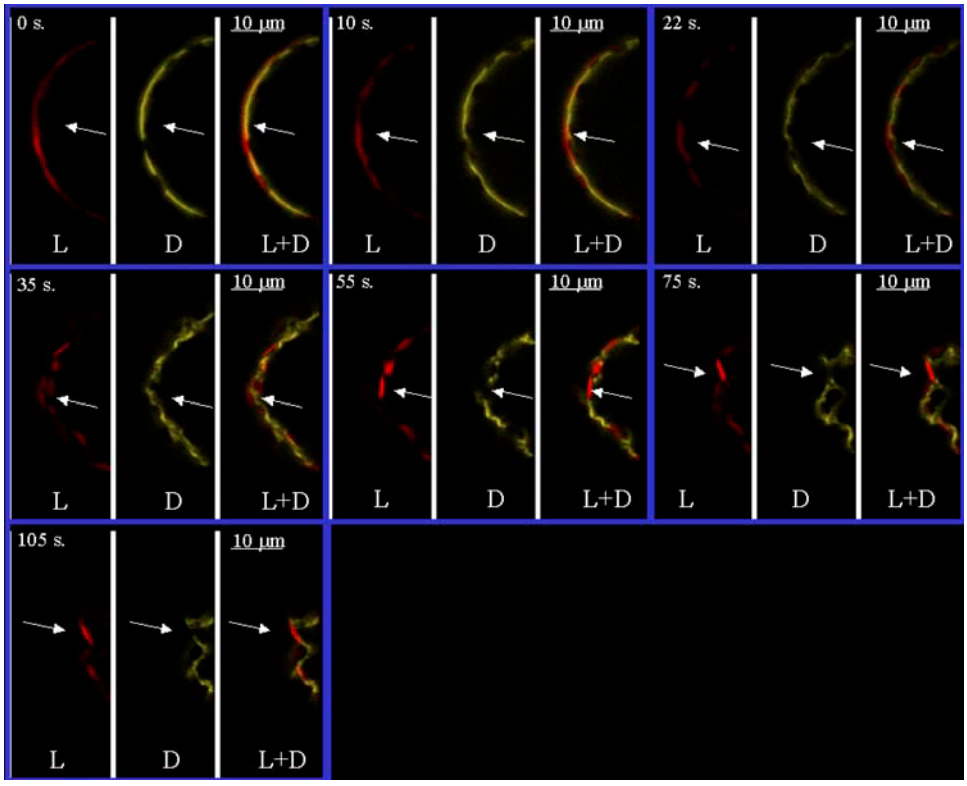

FIGURE 13 Confocal fluorescence microscopy. Time course of the partial solubilization of double-stained vesicles containing 20 mol % Cer. The equatorial planes are shown. Each set of three images contains, respectively, the Laurdan-excited fluorescence (*L*), the DiI fluorescence (*D*), and the corresponding overlap (*L*+*D*). Times after detergent addition are given in seconds. Room temperature. The arrows point to the formation of a large Cer-enriched domain.

Detergent resistance

The observation of a detergent-resistant residue in Triton X-100-treated SM/Cer bilayers (Figs. 1 and 2) is interesting because in studies using vesicles with defined lipid compositions such an effect has only been observed in mixtures containing Ch (and in bilayers composed of pure saturated PCs, well below their T_m) (5). Particularly under our conditions, i.e., large (20:1) molar excess of Triton X-100 and long (24 h) equilibration times, only mixtures containing SM and Ch or certain other sterols have been found to be detergent resistant (12,39). The SM/Cer binary mixture is a welcome addition to the (very limited) collection of detergent-resistant mixtures, because Cer is the end product of SM hydrolysis by sphingomyelinase, thus the mixture is likely to form under certain conditions in the cell membranes. The fact that detergent resistance is not seen with short-chain Cers or with unsaturated phospholipids (Fig. 4) indicates that tight packing of the lipid hydrocarbon chain is essential for the phenomenon to take place. Perhaps the rigidity of Cer chains, whose melting temperature is above 90°C (27,28), and the rigidity of Ch ring exert a comparable effect in giving rise to DRMs, specifically in opposing the insertion of disordered detergent hydrocarbon chains. London and co-workers (39–41) have observed that Cer stabilizes domain formation in SM/PC/Ch mixtures and that Cer displaces Ch from those domains. These authors suggest that tight lipid chain packing is essential for sterol displacement by Cer and for preventing unfavorable contacts between sphingolipid hydrocarbon chains and water. Our results support this hypothesis, underlining in addition the difficulty for detergents to become inserted in ordered domains. A similar situation was found for the solubilization of the tightly packed purple membrane patches in *Halobacterium* membranes (42) and for the case of dimyristoyl PC/Ch bilayers in the liquid-ordered state (11). Our observation of an increased solubilization at temperatures above T_m of the phospholipids (Fig. 5), together with comparable results by Schnitzer et al. (7) and with the observation by Xu et al. (39) of decreased domain formation at comparable temperatures, support equally the notion that tightly packed hydrocarbon lipid chains prevent detergent monomer incorporation.

The data in Figs. 3 and 9–13 reveal that Cer does not only give rise to the phenomenon of detergent resistance but is itself less easily solubilized than SM, so that the nonsolubilized residue is enriched in Cer. This is shown by chemical analysis of the nonsolubilized pellets in Fig. 3 and by the selective loss of the fluorescent SM-rich domains in Fig. 10. Phenomena of preferential solubilization of some lipids have been reported both in cell (43,44) and model (6,45) membranes. However the formation of insoluble domains enriched in Cer that are hardly detectable in the original vesicles but become clearly visible through the detergent action is shown in Figs. 12 and 13 in a particularly clear way. The rigid appearance of the Cer-rich domains, in contrast to the convoluted profiles of the remaining SM-rich areas, is noteworthy as it confirms the predictions based on the Cer physical properties ((13), and references therein).

Implications for cell biology

At least two aspects of this work may be relevant in the context of contemporary cell biology. One is the observation of in-plane separation of Cer-rich and -poor domains, clearly demonstrated in Fig. 9. This, together with the previous spectroscopic and calorimetric evidence (26,27,29,34–37) and our own data in Fig. 6, supports firmly the idea that Cer stabilizes cell membrane ''rafts'' (39,41,46) and induces the formation of large ''platforms'' in plasma membranes (14,47). Note that physiological effects of Cers, e.g., apoptosis, appear to be driven by sphingomyelinase activity (reviews by Cremesti (14) and Futerman and Hannun (16)) and that Cer is precisely the end product of SM hydrolysis by sphingomyelinase, thus our results in model membranes may well mimic the situation in the SM-rich cell plasma membrane upon sphingomyelinase activation.

No less important is the relevance of our results for the interpretation of the findings of DRMs. Membrane fractions resistant to detergent solubilization are often, and not always correctly, identified with cell membrane rafts (3). The dangerous assumption is often made, albeit implicitly, that the detergent-resistant fraction existed as such in the native membrane and that the detergent has not modified it in any significant way. Our results, particularly the images in Figs. 12 and 13, reveal clearly that Cer-rich domains are dramatically enlarged as a result of the preferential solubilization of SM by Triton X-100, i.e., that, at least in our case, the large detergent-resistant domains are partly a detergent artifact. Also interesting is the observation that, beyond a certain temperature, domains melt (Figs. 6–8) (see also Xu et al. (39)) and simultaneously become amenable to solubilization (Fig. 5). The rather common observation in cell biology studies that a DRM fraction is found at 4°C but becomes solubilized at 37°C has been rather puzzling for workers in the area of detergent biophysics, because in principle membranes at higher temperatures should be more and not less resistant to detergent solubilization (6,7), provided that there are no lipid phase changes in that temperature interval. No significant amounts of lipid are found in the cell membranes with a gel-fluid transition temperature above 4°C, with the exception of SM. Most molecular species of SM found in cell membranes have a T_m in the 35°C–40°C range (48). Thus in the SM-rich plasma membrane the conditions exist for the observation of detergent-resistant fractions when the membrane is solubilized at 4°C but not at 37°C.

The authors are grateful to Dr. E. London for pointing out to them the DPH-TEMPO procedure for the detection of ordered domains by fluorescence spectroscopy.

This work was supported in part by grants from the Spanish Ministerio de Educación y Ciencia (No. BFU 2004-02955 to F.M.G., and No.

BMC 2002-00784 to A.A.), and the University of the Basque Country (UPV00042.310/13552 to F.M.G.). Research in the laboratory of LAB is funded by a grant from the Danish Natural Science Research Council (SNF) (21-03-0569) and the Danish National Research Foundation (which supports MEMPHYS-Center for Biomembrane Physics). J.S. is a graduate student supported by the Basque government.

REFERENCES

1. Simons, K., and E. Ikonen. 1997. Functional rafts in cell membranes. *Nature*. 387:569–572.
2. Simons, K., and W. L. Vaz. 2004. Model systems, lipid rafts, and cell membranes. *Annu. Rev. Biophys. Biomol. Struct*. 33:269–295.
3. Lichtenberg, D., F. M. Goñi, and H. Heerklotz. 2005. Detergent-resistant membranes should not be identified with rafts. *Trends Biochem. Sci*. 30:430–436.
4. Schroeder, R., E. London, and D. Brown. 1994. Interactions between saturated acyl chains confer detergent resistance on lipids and glycosylphosphatidylinositol (GPI)-anchored proteins: GPI-anchored proteins in liposomes and cells show similar behavior. *Proc. Natl. Acad. Sci. USA*. 91:12130–12134.
5. Patra, S. K., A. Alonso, and F. M. Goni. 1998. Detergent solubilisation of phospholipid bilayers in the gel state: the role of polar and hydrophobic forces. *Biochim. Biophys. Acta*. 1373:112–118.
6. Sot, J., M. I. Collado, J. L. R. Arrondo, A. Alonso, and F. M. Goñi. 2002. Triton X-100-resistant bilayers: effect of lipid composition and relevance to the raft phenomenon. *Langmuir*. 18:2828–2835.
7. Schnitzer, E., D. Lichtenberg, and M. M. Kozlov. 2003. Temperature-dependence of the solubilization of dipalmitoylphosphatidylcholine (DPPC) by the non-ionic surfactant Triton X-100, kinetic and structural aspects. *Chem. Phys. Lipids*. 126:55–76.
8. Hertz, R., and Y. Barenholz. 1977. Relations between composition of liposomes and their interaction with Triton X-100. *J. Colloid Interface Sci*. 60:188–200.
9. Ipsen, J. H., G. Karlstrom, O. G. Mouritsen, H. Wennerstrom, and M. J. Zuckermann. 1987. Phase equilibria in the phosphatidylcholine-cholesterol system. *Biochim. Biophys. Acta*. 905:162–172.
10. Ahmed, S. N., D. A. Brown, and E. London. 1997. On the origin of sphingolipid/cholesterol-rich detergent-insoluble cell membranes: physiological concentrations of cholesterol and sphingolipid induce formation of a detergent-insoluble, liquid-ordered lipid phase in model membranes. *Biochemistry*. 36:10944–10953.
11. Sáez-Cirión, A., A. Alonso, F. M. Goñi, T. P. W. McMullen, R. N. McElhaney, and E. A. Rivas. 2000. Equilibrium and kinetic studies of the solubilization of phospholipids-cholesterol bilayers by C12E8. The influence of the lipid phase structure. *Langmuir*. 16:1960–1968.
12. Patra, S. K., A. Alonso, J. L. R. Arrondo, and F. M. Goñi. 1999. Liposomes containing sphingomyelin and cholesterol: detergent solubilisation and infrared spectroscopic studies. *J. Liposome Res*. 9:247–260.
13. Kolesnick, R. N., F. M. Goni, and A. Alonso. 2000. Compartmentalization of ceramide signaling: physical foundations and biological effects. *J. Cell. Physiol*. 184:285–300.
14. Cremesti, A. E., F. M. Goni, and R. Kolesnick. 2002. Role of sphingomyelinase and ceramide in modulating rafts: do biophysical properties determine biologic outcome? *FEBS Lett*. 531:47–53.
15. Goñi, F. M., and A. Alonso. 2002. Sphingomyelinases: enzymology and membrane activity. *FEBS Lett*. 531:38–46.
16. Futerman, A. H., and Y. A. Hannun. 2004. The complex life of simple sphingolipids. *EMBO Rep*. 5:777–782.
17. Goñi, F. M., and A. Alonso. 2000. Spectroscopic techniques in the study of membrane solubilization, reconstitution and permeabilization by detergents. *Biochim. Biophys. Acta*. 1508:51–68.
18. Angelova, M. I., and D. S. Dimitrov. 1986. Liposome electroformation. *Faraday Discuss. Chem. Soc*. 81:303–311.
19. Bagatolli, L. A., and E. Gratton. 2000. Two photon microscopy of coexisting lipid domains in giant unilamellar vesicles of binary phospholipid mixtures. *Biophys. J*. 78:290–305.
20. Düzgünes, N., L. A. Bagatolli, P. Meers, Y. Oh, and R. M. Straubinger. 2003. Fluorescence methods in liposome research. *In* Liposomes, 2nd ed. V. P. Torchilin and V. Weissig, editors. Oxford University Press, London. 105–147.
21. Marchesini, N., and Y. A. Hannun. 2004. Acid and neutral sphingomyelinases: roles and mechanisms of regulation. *Biochem. Cell Biol*. 82:27–44.
22. Simon, C. G. Jr., and A. R. Gear. 1998. Membrane-destabilizing properties of C2-ceramide may be responsible for its ability to inhibit platelet aggregation. *Biochemistry*. 37:2059–2069.
23. Sot, J., F. M. Goñi, and A. Alonso. 2005. Molecular associations and surface-active properties of short- and long-N-acyl chain ceramides. *Biochim. Biophys. Acta*. In press.
24. Untracht, S. M., and G. G. Shipley. 1977. Molecular interactions between lecithin and sphingomyelin. Temperature- and composition-dependent phase separation. *J. Biol. Chem*. 252:4449–4457.
25. Ruiz-Arguello, M. B., M. P. Veiga, J. L. Arrondo, F. M. Goni, and A. Alonso. 2002. Sphingomyelinase cleavage of sphingomyelin in pure and mixed lipid membranes. Influence of the physical state of the sphingolipid. *Chem. Phys. Lipids*. 114:11–20.
26. Huang, H. W., E. M. Goldberg, and R. Zidovetzki. 1996. Ceramide induces structural defects into phosphatidylcholine bilayers and activates phospholipase A2. *Biochem. Biophys. Res. Commun*. 220:834–838.
27. Sot, J., F. J. Aranda, M. I. Collado, F. M. Goñi, and A. Alonso. 2005. Different effects of long- and short-chain ceramides on the gel-fluid and lamellar-hexagonal transitions of phospholipids. A calorimetric, NMR and x-ray diffraction study. *Biophys. J*. 88:3368–3380.
28. Shah, J., J. M. Atienza, R. I. Duclos Jr., A. V. Rawlings, Z. Dong, and G. G. Shipley. 1995. Structural and thermotropic properties of synthetic C16:0 (palmitoyl) ceramide: effect of hydration. *J. Lipid Res*. 36:1936–1944.
29. Carrer, D. C., and B. Maggio. 1999. Phase behavior and molecular interactions in mixtures of ceramide with dipalmitoylphosphatidylcholine. *J. Lipid Res*. 40:1978–1989.
30. Florine-Casteel, K., and G. W. Feigenson. 1988. On the use of partition coefficients to characterize the distribution of fluorescent membrane probes between coexisting gel and fluid lipid phase: an analysis of the partition behavior of 1,6-diphenyl-1,3,5-hexatriene. *Biochim. Biophys. Acta*. 941:102–106.
31. Cantor, C. R., and P. R. Schimmel. 1980. Biophysical Chemistry, Part II. Freeman, San Francisco.
32. Chapman, D. 1975. Phase transitions and fluidity characteristics of lipids and cell membranes. *Q. Rev. Biophys*. 8:185–235.
33. Bagatolli, L. A. 2003. Direct observation of lipid domains in free standing bilayers: from simple to complex lipid mixtures. *Chem. Phys. Lipids*. 122:137–145.
34. Massey, J. B. 2001. Interaction of ceramides with phosphatidylcholine, sphingomyelin and sphingomyelin/cholesterol bilayers. *Biochim. Biophys. Acta*. 1510:167–184.
35. Holopainen, J. M., J. Y. Lehtonen, and P. K. Kinnunen. 1997. Lipid microdomains in dimyristoylphosphatidylcholine-ceramide liposomes. *Chem. Phys. Lipids*. 88:1–13.
36. Veiga, M. P., J. L. Arrondo, F. M. Goni, and A. Alonso. 1999. Ceramides in phospholipid membranes: effects on bilayer stability and transition to nonlamellar phases. *Biophys. J*. 76:342–350.
37. Hsueh, Y. W., R. Giles, N. Kitson, and J. Thewalt. 2002. The effect of ceramide on phosphatidylcholine membranes: a deuterium NMR study. *Biophys. J*. 82:3089–3095.
38. Holopainen, J. M., M. Subramanian, and P. K. Kinnunen. 1998. Sphingomyelinase induces lipid microdomain formation in a fluid phosphatidylcholine/sphingomyelin membrane. *Biochemistry*. 37: 17562–17570.
39. Xu, X., R. Bittman, G. Duportail, D. Heissler, C. Vilcheze, and E. London. 2001. Effect of the structure of natural sterols and

sphingolipids on the formation of ordered sphingolipid/sterol domains (rafts). Comparison of cholesterol to plant, fungal, and disease-associated sterols and comparison of sphingomyelin, cerebrosides, and ceramide. *J. Biol. Chem.* 276:33540–33546.

40. Wang, J., Megha, and E. London. 2004. Relationship between sterol/steroid structure and participation in ordered lipid domains (lipid rafts): implications for lipid raft structure and function. *Biochemistry.* 43: 1010–1018.
41. Megha, and E. London. 2004. Ceramide selectively displaces cholesterol from ordered lipid domains (rafts): implications for lipid raft structure and function. *J. Biol. Chem.* 279:9997–10004.
42. Viguera, A. R., J. M. Gonzalez-Manas, S. Taneva, and F. M. Goni. 1994. Early and delayed stages in the solubilization of purple membrane by a polyoxyethylenic surfactant. *Biochim. Biophys. Acta.* 1196:76–80.
43. Yu, J., D. A. Fischman, and T. L. Steck. 1973. Selective solubilization of proteins and phospholipids from red blood cell membranes by non-ionic detergents. *J. Supramol. Struct.* 3:233–247.
44. Gurtubay, J. I., F. M. Goni, J. C. Gomez-Fernandez, J. J. Otamendi, and J. M. Macarulla. 1980. Triton X-100 solubilization of mitochondrial inner and outer membranes. *J. Bioenerg. Biomembr.* 12: 47–70.
45. Urbaneja, M. A., J. L. Nieva, F. M. Goni, and A. Alonso. 1987. The influence of membrane composition on the solubilizing effects of Triton X-100. *Biochim. Biophys. Acta.* 904:337–345.
46. Wang, T. Y., and J. R. Silvius. 2003. Sphingolipid partitioning into ordered domains in cholesterol-free and cholesterol-containing lipid bilayers. *Biophys. J.* 84:367–378.
47. Grassme, H., V. Jendrossek, A. Riehle, G. von Kurthy, J. Berger, H. Schwarz, M. Weller, R. Kolesnick, and E. Gulbins. 2003. Host defense against Pseudomonas aeruginosa requires ceramide-rich membrane rafts. *Nat. Med.* 9:322–330.
48. Barenholz, Y., and T. E. Thompson. 1980. Sphingomyelins in bilayers and biological membranes. *Biochim. Biophys. Acta.* 604: 129–158.